Article

Engrafted Neural Stem/Progenitor Cells Promote Functional Recovery through Synapse Reorganization with Spared Host Neurons after Spinal Cord Injury

Kazuya Yokota,[1,2] Kazu Kobayakawa,[1,2] Kensuke Kubota,[1,2] Atsushi Miyawaki,[3] Hideyuki Okano,[4] Yasuyuki Ohkawa,[5] Yukihide Iwamoto,[1] and Seiji Okada[1,2,*]

[1]Department of Orthopaedic Surgery, Graduate School of Medical Sciences, Kyushu University, 3-1-1 Maidashi, Higashi-ku, Fukuoka 812-8582, Japan
[2]Department of Advanced Medical Initiatives, Graduate School of Medical Sciences, Kyushu University, 3-1-1 Maidashi, Higashi-ku, Fukuoka 812-8582, Japan
[3]Laboratory for Cell Function Dynamics, Brain Science Institute, RIKEN, Saitama 351-0198, Japan
[4]Department of Physiology, Keio University School of Medicine, 35 Shinanomachi, Shinjuku, Tokyo 160-8582, Japan
[5]Department of Advanced Medical Initiatives, JST-CREST, Faculty of Medicine, Kyushu University, 3-1-1 Maidashi, Higashi-ku, Fukuoka 812-8582, Japan
*Correspondence: seokada@ortho.med.kyushu-u.ac.jp
http://dx.doi.org/10.1016/j.stemcr.2015.06.004

SUMMARY

Neural stem/progenitor cell (NSPC) transplantation is a promising therapeutic strategy for spinal cord injury (SCI). However, the efficacy of NSPC transplantation on severe SCI is poorly understood. We herein show that NSPC transplantation promotes functional recovery after mild and moderate SCI, but not after severe SCI. In severe SCI mice, there were few remaining host neurons within the range of NSPC engraftment; thus, we examined whether the co-distribution of transplant and host is a contributory factor for functional improvement. A cellular selective analysis using laser microdissection revealed that drug-induced host neuronal ablation considerably decreased the synaptogenic potential of the engrafted NSPCs. Furthermore, following host neuronal ablation, neuronal retrograde tracing showed less propriospinal relay connections bridging the lesion after NSPC transplantation. Our findings suggest that the interactive synaptic reorganization between engrafted NSPCs and spared host neurons is crucial for functional recovery, providing significant insight for establishing therapeutic strategies for severe SCI.

INTRODUCTION

Traumatic spinal cord injury (SCI) results in the death of neural cells and a disruption of interneuronal connectivity with sensory/motor functional deficits (Bradbury and McMahon, 2006). Notably, severe SCI patients suffer from permanent complete paraplegia, which imposes considerable mental and economic burdens compared with those of patients with mild and moderate SCI (Coleman et al., 2015; Krueger et al., 2013). Therefore, there is a great demand for developing therapeutic approaches, particularly for severe SCI.

The transplantation of stem cells for SCI, such as neural stem/progenitor cells (NSPCs), is a promising therapeutic approach to alleviate the inflammatory response and replace lost neural cells (Volarevic et al., 2013). This stem cell-based strategy has been shown to have therapeutic evidence for SCI in many experimental animals (Mothe and Tator, 2013; Tetzlaff et al., 2011). However, most studies have shown that NSPC transplantation promoted functional recovery following mild and moderate SCI, while its therapeutic efficacy for severe SCI has been unclear, and the detailed mechanism underlying such efficacy still remains to be elucidated.

In contrast to severe SCI, varying degrees of spontaneous recovery are observed following mild and moderate SCI in both humans and experimental animals (Bareyre et al., 2004; Kobayakawa et al., 2014). Such recovery is attributed to the endogenous plasticity of neural circuits, which means that propriospinal relay connections bypass the lesions (Courtine et al., 2008). A neurobiological approach toward enhancing the propriospinal relay connections could be a therapeutic option for SCI. However, little is known about whether transplanted NSPCs integrate into the spared neural circuits and reassemble the propriospinal relay connections. In the present study, we thus focused on the synaptogenic potential of engrafted NSPCs and the reorganization of the propriospinal circuits after transplantation.

Conventional methods for assessing the cellular properties of the engrafted NSPCs mainly have relied on histological examinations (Abematsu et al., 2010; Nori et al., 2011), and there have been few methods available to analyze the in vivo function of NSPCs in the injured spinal cord. To obtain a detailed understanding of the synaptogenic potential of the engrafted NSPCs, it is necessary to develop a method to quantify the molecular properties of NSPCs in situ. We applied laser microdissection (LMD), which is a powerful tool for isolating specific cell types from heterogeneous tissues, to investigate the transcriptional activity of engrafted NSPCs.

In this study, we examined the effects of NSPC transplantation on the functional recovery of mice with different

severities of contusion SCI. Physiological and histological analyses revealed that NSPC transplantation failed to promote the functional recovery of the animals with severe SCI, even though the NSPCs were suitably grafted and differentiated into neural cells. In addition, we investigated whether the drug-induced ablation of host neurons influenced the effects of NSPC transplantation, including the reorganization of neural circuits, synaptogenesis, and functional improvement, in animals with moderate SCI. Our findings suggest that the spatial interactions and synaptic contacts between engrafted NSPCs and spared host neurons are crucial for functional recovery following SCI.

RESULTS

NSPC Transplantation Improved the Functional Recovery for the Mice with Mild and Moderate SCI, but Not with Severe SCI

To examine whether NSPC transplantation improves the functional recovery, irrespective of the severity of SCI, we first produced a mouse SCI model with three different severities of the injury, mild (50 kdyn), moderate (70 kdyn), and severe (90 kdyn), at the ninth thoracic level using an Infinite Horizons impactor. In these groups, both the actual impact force and the calculated displacement were highly reproducible, and there was a strong linear relationship between the actual impact force and the measured displacement (Pearson: force versus displacement, R = 0.9591, p < 0.0001) (Figure 1A). After confirming the reproducibility of the SCI, we transplanted 5×10^5 NSPCs into the lesion epicenter immediately after injury at the ninth thoracic level in all groups. The hindlimb locomotor recovery was assessed using the Basso Mouse Scale (BMS) open-field motor score, footprint analysis, and grip walk test. At 6 weeks after transplantation, better functional recovery was observed in the mild and moderate SCI groups compared to that observed in the medium-injected control groups. In contrast, the functional recovery was comparable between the severe SCI group and the control group in all physiological examinations (Figures 1B–1E).

To examine whether this difference in the efficacy of functional improvement could be attributed to differences in graft survival, we tracked the cell viability using a bioluminescence imaging system that detects luciferase photon signals only from living cells. However, this analysis showed comparable signal intensity among all groups at 6 weeks after transplantation (Figures S1A and S1B). In addition, immunohistochemical analyses demonstrated that the fractions of differentiated HU-positive neurons, APC-positive oligodendrocytes, and GFAP-positive astrocytes from the engrafted NSPCs were similar in all groups (Figures S1C and S1D). These results suggest that the graft

survival and the differentiation phenotypes were not significantly affected by the severity of SCI. Regarding the distribution of engrafted NSPCs, histopathological examinations showed that the engrafted cells were located within a range of approximately 2 mm rostral and caudal to the lesion epicenter in all groups, and we did not identify any significant differences in the spatial distribution of NSPCs among the three groups (Figures S1E and S1F).

As previously reported, the features of acute inflammation triggered by SCI, such as the production of proinflammatory cytokines and reactive oxygen species, are important factors that modulate the microenvironment of the injured spinal cord (Cusimano et al., 2012; Nishimura et al., 2013). Because the extent of inflammatory reactions is proportional to the severity of SCI, we speculated that the differences in inflammatory reactions could negate the efficacy of the engrafted NSPCs and, thus, result in a comparable functional recovery between the NSPC-transplantation group and the control group after severe SCI. To rule out this possibility, we transplanted the same number of NSPCs into the injured spinal cord at 7 days after SCI, when the inflammatory reactions were resolved in all groups. However, NSPC transplantation, even in the subacute phase, did not significantly improve the functional recovery in the severe SCI group, while the mild and moderate SCI groups showed a better functional recovery than the medium-injected control groups (Figures 1F and S2A–S2C; Okada et al., 2005). This difference of recovery in subacute phase also was not attributed to the graft survival or differentiation phenotypes (Figures S2D and S2E). In addition, even in the CD11b-depleted mice (through the administration of anti-Gr-1 antibody) and in non-obese diabetic/severe combined immunodeficiency (NOD/SCID) mice, NSPC transplantation did not promote functional recovery after severe SCI (data not shown). These results together suggest that the ineffectiveness of NSPC transplantation in the severe SCI group was not due to poor graft survival, the differentiation phenotypes, the distribution of engrafted NSPCs, or the inflammatory reactions of the injured spinal cord.

Selective Ablation of Host Neurons around the Lesion Area Negates the Functional Improvement after NSPC Transplantation Even after Moderate SCI

To examine the cause of the ineffectiveness of NSPC transplantation in the severe SCI group, we performed histological analyses focusing on the differences in the distribution of the spared host neurons associated with engrafted NSPCs among the three SCI groups. In all groups, double immunofluorescence analyses showed that CD11b-positive inflammatory cells had markedly infiltrated into the lesion epicenter at 7 days after SCI, and that the infiltrating area was proportional to the severity
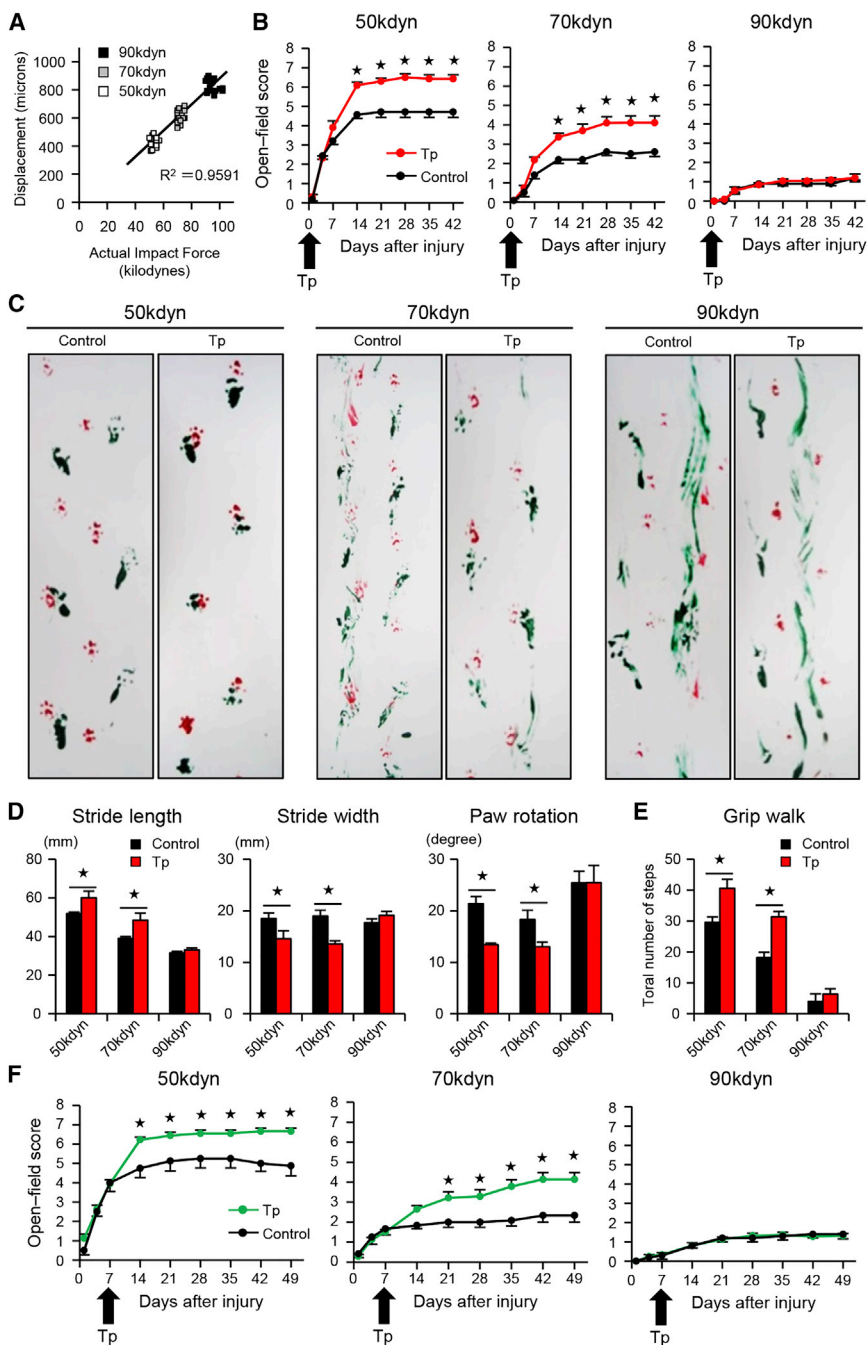
Figure 1. Effects of NSPC Transplantation in the Mild, Moderate, and Severe SCI Groups

(A) The correlation between the actual impact force and calculated displacement in the mild (50 kdyn), moderate (70 kdyn), and severe (90 kdyn) SCI groups is shown (n = 12–14 mice per group; p < 0.0001, Pearson correlation coefficient).

(B) The time course of the functional recovery based on the BMS score in the acute NSPC transplantation groups and control groups is shown (n = 12–14 mice per group).

(C–E) The results of the footprint analyses and grip walk test of the mice with SCI in the NSPC transplantation and control groups at 6 weeks after transplantation are shown (n = 8 mice per group).

(F) The time course of the functional recovery based on the BMS score in the subacute NSPC transplantation and control groups is shown (n = 12–14 mice per group).

*p < 0.05 versus control, two-way repeated-measures ANOVA with the Tukey-Kramer post hoc test (B and F) or Wilcoxon rank-sum test (D and E). The data are presented as the means ± SEM.

See also Figures S1 and S2.

of SCI. Meanwhile, most NEUN-positive neurons were spared outside the CD11b-positive infiltrating area, and the area of neuronal loss also was proportional to the SCI severity. Notably, in the severe SCI group, there were few remaining neurons within the area approximately 2 mm rostral and caudal to the lesion epicenter (Figures 2A and 2B). Considering that the NSPC engraftment was not affected by severity of SCI (Figure S1E), the transplanted NSPCs were mostly integrated into this area of neuronal loss in the severe SCI group, while there were a number of remaining neurons within the area of NSPC engraftment in the mild and moderate SCI groups. These results led us to hypothesize that the co-distribution of the engrafted NSPCs with the spared host neurons is crucial for the functional improvement after NSPC transplantation.

To verify this hypothesis, we performed selective ablation of host neurons by injecting the axon-sparing
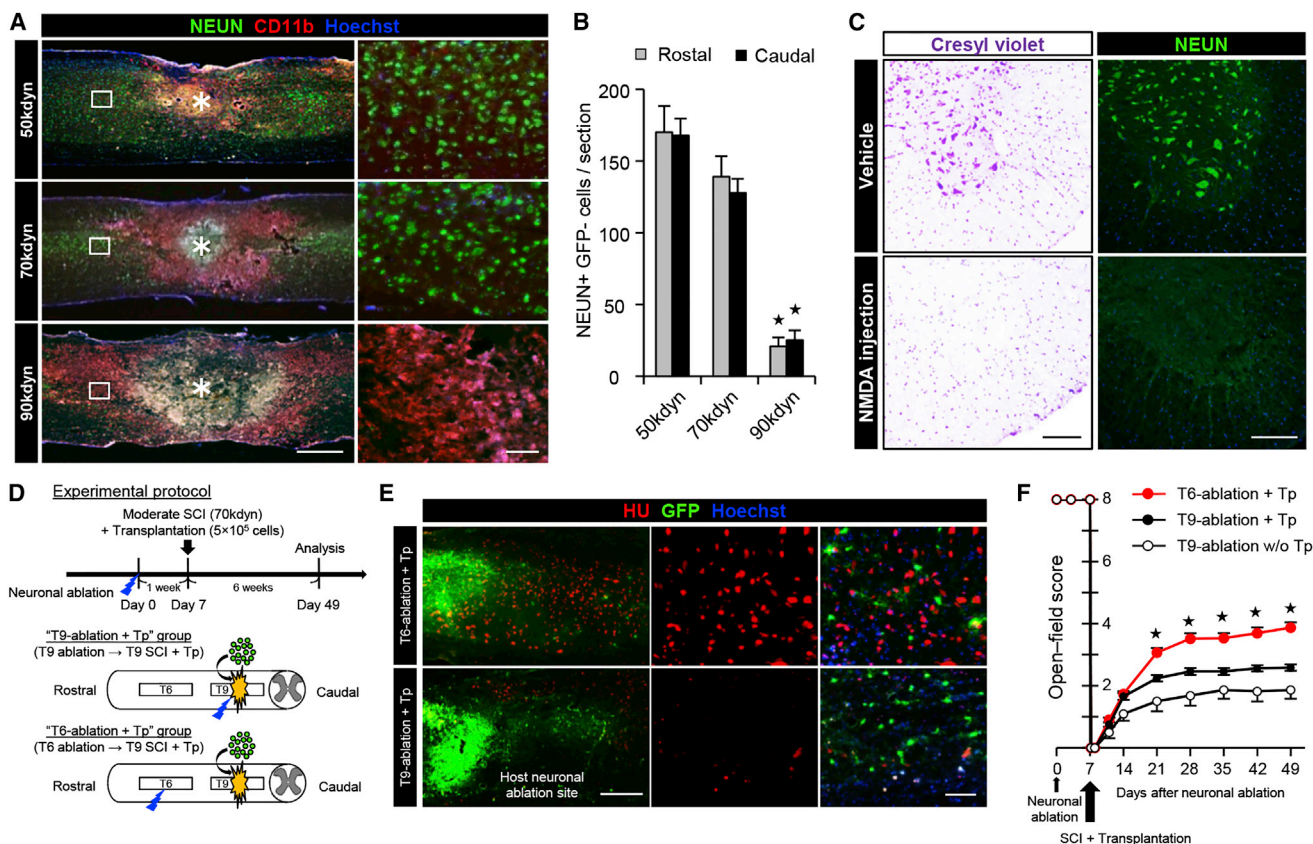
Figure 2. Selective Host Neuronal Ablation Negates the Efficacy of NSPC Transplantation

(A) The results of an immunohistochemical analysis of the spared host neurons and inflammatory cells at 7 days after SCI, where cells were stained with NEUN (green), CD11b (red), and Hoechst (blue). The asterisk indicates the lesion epicenter. The right images are magnifications of the boxed areas in the left images.

(B) Quantification of the number of NEUN-positive cells 1 mm distant from the lesion epicenter is shown (n = 8 mice per group).

(C) Cresyl violet staining and immunohistochemical staining for anti-NEUN revealed a pronounced loss of spinal cord neurons induced by NMDA injection.

(D) The schedule of SCI and NSPC transplantation with host neuronal ablation is shown.

(E) The results of an immunohistochemical analysis of the GFP (green) and HU (red) staining at 6 weeks after transplantation are shown.

(F) The time course of the functional recovery in the T6-ablation + Tp group, the T9-ablation + Tp group, and the T9-ablation without Tp group is shown (n = 8–12 mice per group).

*p < 0.05 versus other groups, Dunnett's test (B) or two-way repeated-measures ANOVA with the Tukey-Kramer post hoc test (F). The data are presented as the means ± SEM. Scale bars, 500 μm (A), 100 μm (insets), 50 μm (C), 500 μm (E, left), and 50 μm (E, right).

See also Figure S3.

excitotoxin, N-methyl-D-aspartic acid (NMDA), into the spinal cord. This NMDA injection ablated the spinal cord neurons, including interneurons and motor neurons, at the level of each injection (Figure 2C); however, it had little effect on myelinated long-descending fiber tracts or on the hindlimb motor function, in agreement with the previous findings by another group (Courtine et al., 2008). In addition, immunohistochemistry and qRT-PCR analyses showed that an inflammatory reaction by NMDA injection was not observed in the host spinal cord at 1 week after injection (Figures S3A and S3B). The experimental protocol is

shown in Figure 2D; 7 days after neuronal ablation by NMDA injection at the ninth or sixth thoracic level, we produced the moderate SCI (70 kdyn) at the ninth thoracic level and transplanted 5 × 10⁵ NSPCs into the lesion epicenter immediately after SCI. In the T9-ablation + Tp group, the SCI and NSPC transplantation were performed at the same level as the neuronal ablation, whereas in the T6-ablation + Tp group, the SCI and transplantation were performed at a level distant from the neuronal ablation area. Thus, the co-distribution between spared host neurons and the engrafted NSPCs was hardly observed in the
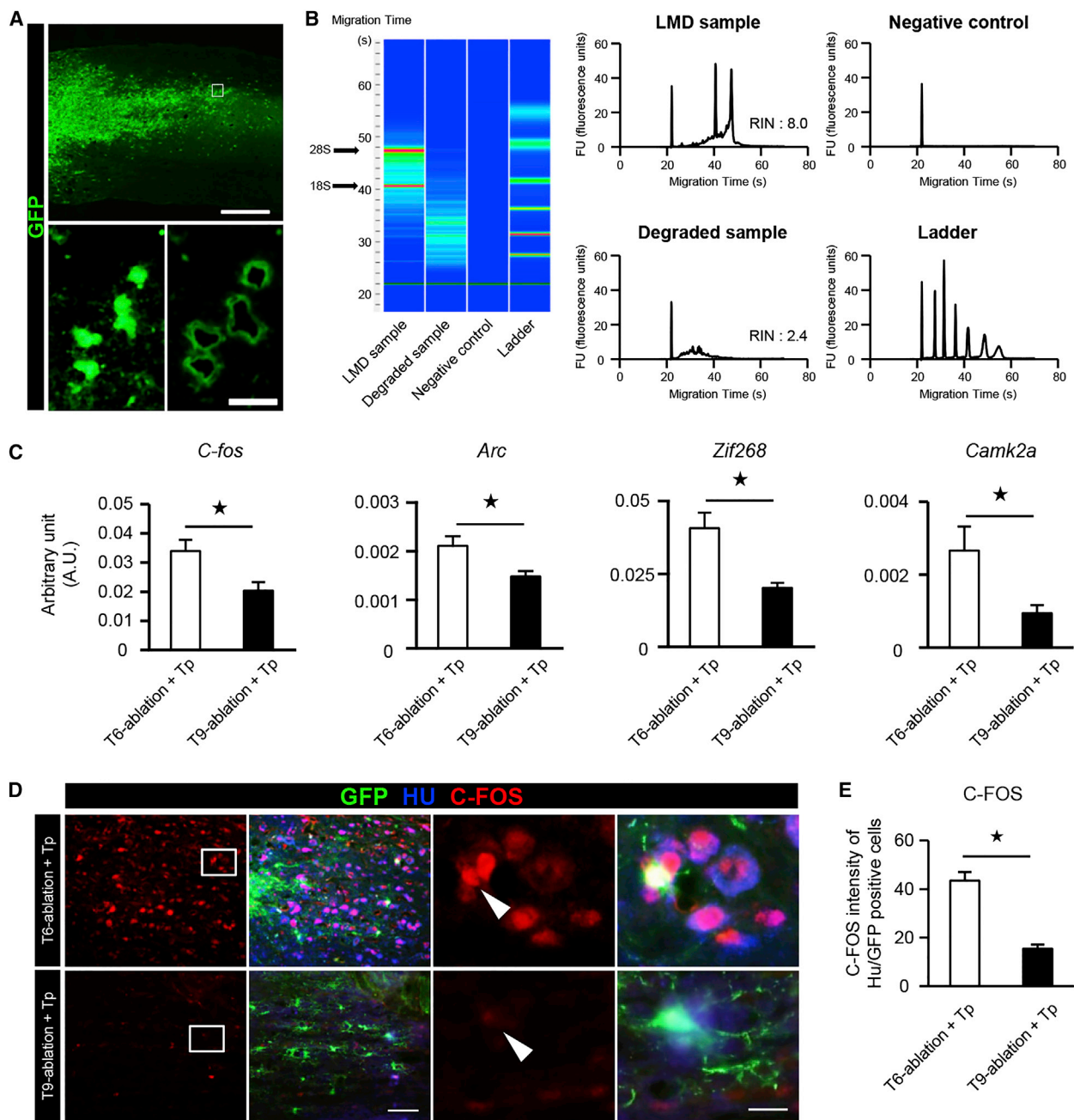
Figure 3. The Neuronal Activity of Engrafted NSPCs Was Significantly Decreased in the Absence of Spared Host Neurons

(A) The results of an immunohistochemical analysis of GFP-positive engrafted NSPCs at 6 weeks after transplantation. The lower left image (before LMD) and right image (after LMD) are magnifications of the bowed areas in the upper image.

(B) The RNA quality was confirmed by a bioanalyzer with the RNA integrity number (RIN).

(C) The gene expression levels of neuronal activity markers in engrafted NSPCs at 6 weeks after transplantation, as determined by qRT-PCR, are shown (n = 8 mice per group).

(D) Triple immunostaining for GFP (green), C-FOS (red), and HU (blue) at 6 weeks after transplantation. The images showed that lower C-FOS expression was observed in GFP/HU-positive neurons (arrowhead) in the T9-ablation + Tp group compared to the T6-ablation + Tp group. The right images are magnifications of the boxed areas in the left images.

(legend continued on next page)

T9-ablation + Tp group, but was kept intact in the T6-ablation + Tp group, as shown in Figure 2E. During the first week after injury, the functional recovery in both groups was comparable; however, there was a significant difference between the two groups beginning the following week (Figure 2F). Meanwhile, in the T9-ablation + Tp group, the open-field motor score at 6 weeks after SCI was equivalent to that of the group with SCI without NSPC transplantation (Figure 1B), thereby indicating that the preconditioning involving host neuronal ablation at the area of engraftment negated the efficacy of NSPC transplantation. These data suggest that the spatial interaction between the engrafted NSPCs and the spared host neurons plays a crucial role in the efficacy of NSPC transplantation after SCI.

The Neuronal Activity of Engrafted NSPCs Was Significantly Decreased in the Absence of Spared Host Neurons

Next, to examine the cause of the ineffectiveness of NSPC transplantation in the setting of T9-neuronal ablation, we evaluated the differences in the distribution, the differentiation phenotypes, and the neuronal activity of the engrafted NSPCs between the T9-ablation + Tp group and the T6-ablation + Tp group. In the immunohistochemical analysis, we confirmed that the distribution of the engraftment of GFP-positive cells was comparable in both groups (Figures S4A and S4B). With regard to differentiation, the ratio of GFP/HU-positive neurons to GFP-positive cells also was similar between the two groups (Figure S4C). We therefore speculated that the in vivo function, such as the neuronal activity of the engrafted NSPCs, could be altered by the graft environmental setting.

To examine the in vivo functions of the engrafted NSPCs, we identified large GFP-positive neurons under a fluorescence microscope and selectively isolated them by LMD at 6 weeks after transplantation (Figure 3A). RNA was prepared from the captured cells in both groups, and excellent RNA qualities were confirmed by a bioanalyzer that provided the RNA integrity number (RIN). Each LMD sample showed intact 18S rRNA/28S rRNA bands in an electrophoretic analysis, whereas a degraded sample of heat-denatured RNA showed no 18S rRNA/28S rRNA bands (Figure 3B), which indicated that the RNA samples obtained through LMD were reliable and could be used for RT-PCR analyses. We confirmed the gene expression of the neuronal markers, such as *Tubb3*, *Ascl1*, *Dcx*, *Neurod1*,

Map2, and *Gap43*, rather than glial cell markers, such as *Cnpase* (oligodendrocyte) and *Gfap* (astrocyte), in the isolated NSPCs by RT-PCR, indicating that the GFP-positive cells isolated by LMD were mostly neuronal cells (Figures S4D–S4F). The expression levels of neuronal differentiation markers and neurite growth markers were comparable in the engrafted NSPCs in the T9-ablation + Tp and T6-ablation + Tp groups (Figures S4E and S4F). Notably, the gene expression levels for the markers of neuronal activity, such as *C-fos*, *Arc*, *Zif268*, and *Camk2a*, were significantly decreased in the T9-ablation + Tp group (Figure 3C). Consistent with the gene expression, a significant decrease in C-FOS protein expression in the engrafted NSPCs was confirmed by an immunofluorescence analysis at 6 weeks after transplantation (Figures 3D and 3E). These markers of neuronal activity are essential for establishing neural connectivity and evoking action potentials in neuronal cells (Flavell and Greenberg, 2008); therefore, the decreased expression of these markers in the engrafted NSPCs likely resulted in the impaired functional recovery even for the moderate SCI group.

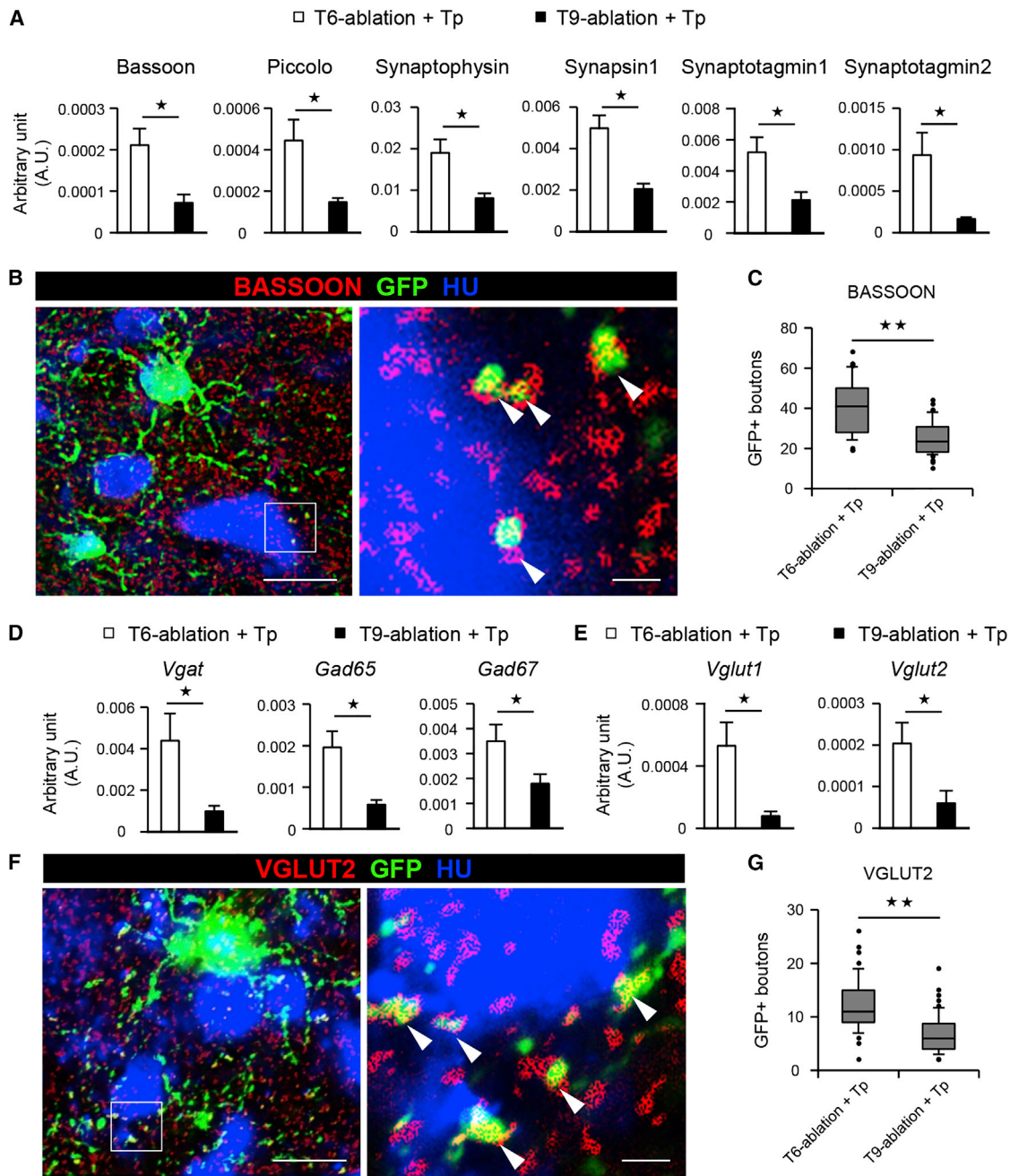### Engrafted NSPCs Form Synaptic Connectivity with Spared Host Neurons after SCI

Because the neuronal activity is associated with the efficacy of synaptic transmission (Südhof, 2013), we compared the differences in the expression of synaptic molecules in the engrafted NSPCs between the T9-ablation + Tp group and the T6-ablation + Tp group. In both groups, a qRT-PCR analysis demonstrated that the engrafted NSPCs expressed presynaptic molecules, such as Bassoon, Piccolo, Synaptophysin, Synapsin1, Synaptotagmin1, and Synaptotagmin2 (Figure 4A). In addition to the gene expression profiles, an immunofluorescence analysis showed that the GFP-positive engrafted NSPCs expressed presynaptic BASSOON molecules in their axonal terminals, which surrounded the HU-positive host neurons (Figure 4B). Quantitative analyses showed that the gene expression levels of these presynaptic molecules, as well as the number of GFP/BASSOON-positive synapses, were significantly lower in the T9-ablation + Tp group compared to those in the T6-ablation + Tp group (Figures 4A–4C).

In most of the previous reports, the engrafted neural stem cells in the injured spinal cord were differentiated into the inhibitory interneurons (Cummings et al., 2005; Nori et al., 2011). In the present study, we also confirmed the expressions of gene-encoding inhibitory presynaptic molecules,

(E) The result of a comparison of the C-FOS intensity in GFP/HU-positive neurons between the T6-ablation + Tp group and the T9-ablation + Tp group is shown (n = 8 mice per group).

*p < 0.05, Wilcoxon rank-sum test (C and E). The data are presented as the means ± SEM. Scale bars, 300 μm (A), 20 μm (insets), 100 μm (D), and 20 μm (insets).

See also Figure S4.

Figure 4. Engrafted NSPCs Form Presynaptic Connectivity with Spared Host Neurons after SCI

(A) The gene expression levels of pan-presynaptic markers in engrafted NSPCs at 6 weeks after transplantation, as determined by qRT-PCR, are shown (n = 8 mice per group).

(B) Triple-staining for GFP (green), HU (blue), and the presynaptic marker BASSOON (red) at 6 weeks after transplantation. The images showed that the engrafted NSPCs expressed BASSOON-positive synaptic boutons (arrowhead) in their axon terminals, which surrounded HU-positive host neurons. The right image is a magnification of the boxed area in the left image.

(C) Quantification of the GFP/BASSOON-positive synaptic boutons in engrafted NSPCs is shown (n = 60 neurons; six mice per group).

(D and E) The gene expression levels of inhibitory presynaptic markers (*Vgat*, *Gad65*, and *Gad67*) and excitatory presynaptic markers (*Vglut1* and *Vglut2*) in engrafted NSPCs at 6 weeks after transplantation, as determined by qRT-PCR, are shown (n = 8 mice per group).

(legend continued on next page)

such as *Vgat*, *Gad65*, and *Gad67*, in the engrafted NSPCs in both groups. However, a qRT-PCR analysis showed that the expression levels of these presynaptic markers were significantly lower in the T9-ablation + Tp group compared to the T6-ablation + Tp group (Figure 4D). In addition to the inhibitory presynaptic molecules, we found that excitatory presynaptic molecules, such as *Vglut1* and *Vglut2*, were expressed in the engrafted NSPCs, and their gene expression levels were significantly different between the two groups (Figure 4E). Differentiated neurons expressing both inhibitory and excitatory molecules were rarely observed (data not shown). An immunofluorescence analysis confirmed the expression of VGLUT2 in the GFP-positive axonal terminals at the border of the host neurons. Consistent with the results of the qRT-PCR analysis, a significantly smaller number of GFP/VGLUT2-positive synapses were observed in the T9-ablation + Tp group than in the T6-ablation + Tp group (Figures 4F and 4G). These results clearly show that the engrafted NSPCs could protrude axons and form both inhibitory and excitatory synapses with the host neurons in the injured spinal cord, and that the graft environment significantly affects the expression of presynaptic molecules in the engrafted NSPCs.

To form relay connections between the graft and host neurons, the engrafted NSPCs are required to express postsynaptic molecules as well as presynaptic molecules. Thus, we next evaluated the expression of postsynaptic molecules in the engrafted NSPCs. In both groups, we observed the gene expression of postsynaptic molecules, such as *Psd95*, Homer1, and Shank1, in the engrafted NSPCs (Figure 5A). Notably, an immunohistochemical analysis showed that the engrafted NSPCs appeared to express PSD95 and HOMER1 in their neurites (Figure 5B). A quantitative analysis revealed that significantly lower gene expression levels of *Psd95*, Homer1, and Shank1 were observed in the T9-ablation + Tp group compared to the T6-ablation + Tp group. Furthermore, the numbers of GFP/PSD95-positive and GFP/HOMER1-positive postsynaptic molecules in the engrafted NSPCs were significantly lower in the T9-ablation + Tp group than in the T6-ablation + Tp group (Figures 5C and 5D). These results indicate that the engrafted NSPCs not only transmit the synaptic signals to the spared host neurons, but also receive the synaptic inputs from the spared host neurons. Considering the differences in the expression levels of presynaptic and postsynaptic molecules in the engrafted

NSPCs between the two groups, it appears that the co-distribution of the engrafted NSPCs with spared host neurons is essential for the formation of synaptic relays after NSPC transplantation.

NSPC Transplantation Promotes the Reorganization of Propriospinal Circuits after SCI

After confirming that the engrafted NSPCs formed synaptic connectivity with spared host neurons (Figures 4 and 5), we next examined the effects of NSPC transplantation on the reassembly of spinal propriospinal circuits. The propriospinal circuit is an indirect descending neural circuit connecting the spinal cord neurons (Flynn et al., 2011). To assess the extent of the reorganization of propriospinal circuits after SCI, we performed retrograde *trans*-synaptic tracing with a rhodamine tracer dye. The experimental protocol is shown in Figure 6A. At 6 weeks after the ninth thoracic SCI, we injected the tracer into the left second lumbar spinal cord, and at 7 days after tracer injection, we quantitated the number of labeled neurons at the ipsilateral (the same side as the tracer injection) and contralateral (the side opposite the tracer injection) fourth thoracic spinal cord. First, in a naive spinal cord, we confirmed that the tracer was captured selectively into the neuronal cell body when using our experimental protocol (Figure 6B). We then compared the number of labeled neurons among the three SCI groups: the T9-ablation + Tp group (SCI plus NSPC transplantation after T9-neuronal ablation), the T6-ablation + Tp group (SCI plus NSPC transplantation after T6-neuronal ablation), and the SCI only group (SCI without NSPC transplantation and neuronal ablation).

A histopathological analysis demonstrated that the number of labeled neurons was significantly greater in the T6-ablation + Tp group compared to the SCI only group, suggesting that NSPC transplantation promoted the reorganization of propriospinal circuits after SCI. Meanwhile, the number of labeled neurons in the T9-ablation + Tp group was significantly lower than that observed in either the T6-ablation + Tp group or the SCI only group (Figures 6C and 6D). These results indicate that the spared host neurons in the vicinity of the lesion area play an important role in the reorganization of propriospinal circuits, even without NSPC transplantation and all the more so with NSPC transplantation after SCI. In fact, as shown in the bottom line in Figure 2F, neuronal ablation at the site of SCI prevented a spontaneous functional recovery. Because

(F) Triple-staining for GFP (green), HU (blue), and the excitatory presynaptic marker VGLUT2 (red) at 6 weeks after transplantation. The images showed that the GFP/VGLUT2-positive excitatory synaptic boutons (arrowhead) contacted HU-positive host neurons. The right image is a magnification of the boxed area in the left image.
(G) Quantification of the GFP/VGLUT2-positive synaptic boutons in engrafted NSPCs is shown (n = 60 neurons; six mice per group).
*p < 0.05, **p < 0.0001, Wilcoxon rank-sum test (A, C, D, E, and G). The data are presented as the means ± SEM. Scale bars, 20 μm (B and F) and 2 μm (insets).
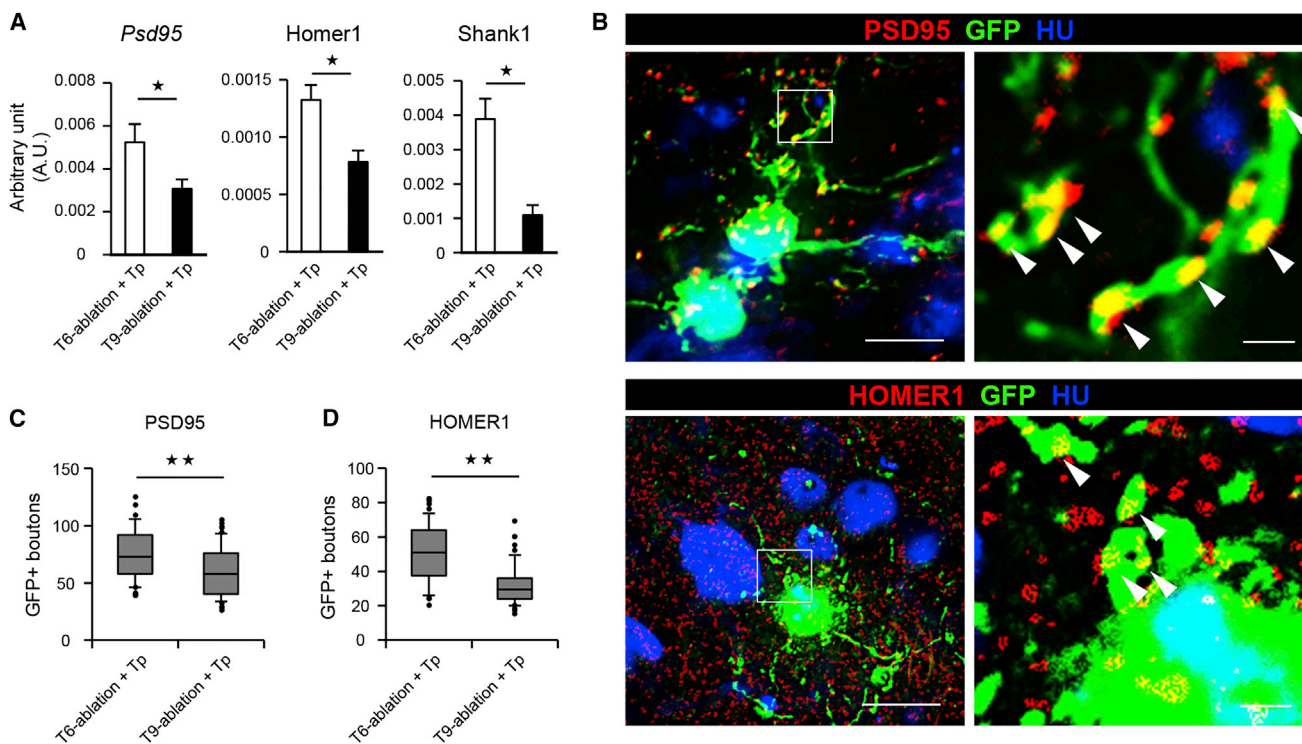
Figure 5. Engrafted NSPCs Form Postsynaptic Connectivity with Spared Host Neurons after SCI

(A) The gene expression levels of postsynaptic markers in engrafted NSPCs at 6 weeks after transplantation, as determined by qRT-PCR, are shown (n = 8 mice per group).

(B) Triple staining for GFP (green), HU (blue), and the postsynaptic marker PSD95 or HOMER1 (red) at 6 weeks after transplantation. The images showed that engrafted NSPCs expressed PSD95-positive or HOMER1-positive synaptic boutons (arrowhead) in their dendrites. The right images are magnifications of the boxed areas in the left images.

(C and D) Quantification of the GFP/PSD95-positive and GFP/HOMER1-positive postsynaptic boutons in engrafted NSPCs is shown (n = 60 neurons; six mice per group).

*p < 0.05, **p < 0.0001, Wilcoxon rank-sum test (A, C, and D). The data are presented as the means ± SEM. Scale bars, 20 μm (B) and 2 μm (insets).

contralateral labeling involves more polysynaptic transmission than ipsilateral labeling (Shah et al., 2013), we assumed that there would be few labeled neurons in the contralateral side in our experimental models. However, we observed some labeled neurons contralaterally in the T6-ablation + Tp group (Figures 6C and 6D), suggesting that NSPC transplantation promotes the reorganization of propriospinal circuits not only in the longitudinal direction, but also in the transverse direction.

DISCUSSION

In this study, we demonstrated three significant findings. First, the degree of severity of the SCI affects the efficacy of NSPC transplantation for promoting functional recovery after SCI. Following mild and moderate SCI, NSPC transplantation significantly improved the locomotor

functional recovery, but this was not the case after severe SCI. Second, engrafted NSPCs must be integrated into the host propriospinal circuits in order to achieve a functional improvement after SCI. Drug-induced selective ablation of host neurons abolished the efficacy of NSPC transplantation even after moderate SCI. In the severely injured spinal cord, there were very few remaining host neurons within the range of NSPC engraftment, which was considered to be one cause of the failure to achieve a better functional recovery after NSPC transplantation. Finally, the selective analysis for the in vivo function of engrafted NSPCs by LMD revealed that the synaptic integration between the engrafted NSPCs and the host neurons is important for the reassembly of propriospinal circuits. These results provide evidence of the therapeutic mechanism underlying interactive synaptic reorganization after NSPC transplantation, and they also suggest the significance of developing an NSPC-based strategy tailored to the severity of SCI.
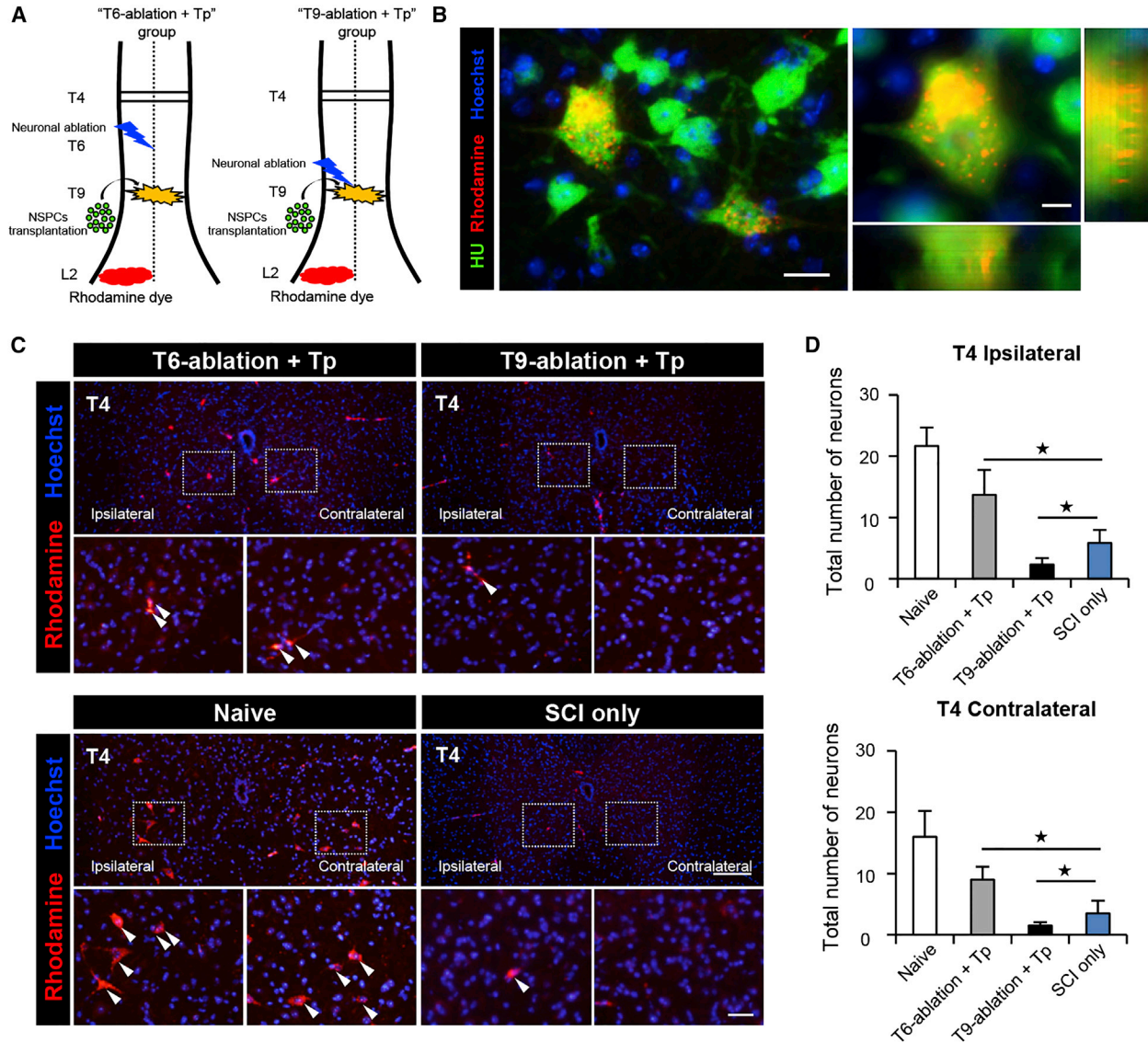
Figure 6. NSPC Transplantation Promotes the Reorganization of Propriospinal Circuits after SCI

(A) A schematic illustration shows the sites of dye injection at the second lumbar spinal cord, the neuronal ablation at the sixth or ninth thoracic spinal cord, and the contusion SCI plus NSPC transplantation at the ninth thoracic spinal cord.

(B) The immunohistochemical analysis showed that HU-positive neurons (green) captured rhodamine tracer dye (red) at 7 days after tracer injection in a naive spinal cord.

(C) The immunohistochemical analysis showed rhodamine-positive (red) retrogradely labeled neurons in the Naive group, the T6-ablation + Tp group, the T9-ablation + Tp group, and SCI only group at the fourth thoracic spinal cord segments. The lower images are magnifications of the boxed areas in the upper images.

(D) The results of a comparison of the number of rhodamine-positive retrogradely labeled neurons are shown (n = 6 mice per group).

*p < 0.05, ANOVA with the Tukey-Kramer post hoc test (D). The data are presented as the means ± SEM. Scale bars, 20 μm (B, left), 5 μm (B, right), 100 μm (C), and 20 μm (insets).

The mechanisms underlying the functional improvement after NSPC transplantation remain unexplained, which has hampered the establishment of therapeutic protocols for the treatment of SCI (Lindvall and Kokaia, 2010). Several possible explanations for the efficacy of the en-grafted NSPCs have been suggested, such as neural cell replacement, remyelination, growth support, neuroprotection, and immunomodulation (Volarevic et al., 2013). However, little is known about the therapeutic effects of the engrafted NSPCs on the disrupted local neural

networks in the injured spinal cord. In this study, we focused on the propriospinal system, the intraspinal neural networks connecting each spinal cord segment (Flynn et al., 2011). This system has received a lot of attention as being important for spontaneous functional recovery after incomplete SCI. For example, Courtine and colleagues demonstrated that a pronounced functional recovery occurred following the spontaneous reorganization of propriospinal circuits without the restoration of the direct projections from the brain to the spinal motor neurons in a rat model of incomplete SCI. Because the extent of spontaneous recovery after SCI is associated with the amount of spared propriospinal circuits, little functional recovery was observed after severe SCI, in which there were few spared host neurons and spared propriospinal circuits (Figures 1 and 2; Conta and Stelzner, 2004; Courtine et al., 2008). In this paper, we showed that the reorganization of propriospinal circuits was promoted by the engrafted NSPCs through synapse formation between the engrafted NSPCs and the host neurons (Figures 4, 5, and 6). In addition, selective ablation of the host neurons abolished the synaptogenic potential of the engrafted NSPCs and negated the efficacy of the reorganization of propriospinal circuits. These results suggest the importance of functional improvement due to the accelerated reorganization of propriospinal circuits by NSPC transplantation after SCI. Indeed, the most prominent effect of NSPC transplantation was observed within 2 weeks after transplantation, and this phase was consistent with the spontaneous recovery process in the control groups (Figure 1).

To date, fluorescence-activated cell sorting (FACS) or translating ribosomal affinity purification (TRAP) techniques mainly have been used for cell-specific profiling of engrafted cells (Doyle et al., 2008; Lobo et al., 2006). Although these techniques have broad utility, the LMD procedure provided several advantages over these methods in this study. First, LMD makes it possible to capture neuronal cells even in the adult CNS. FACS and TRAP are not recommended for the analysis of mature neural tissues, because myelin and tight extracellular matrix proteins interfere with the isolation of neurons. To apply FACS and TRAP to isolate neuronal cells from the adult CNS, enzymatic dissociation is required to eliminate these interfering substances; however, this enzymatic method often results in a loss of cells, including their mRNAs and proteins (Garg et al., 2014). Second, LMD enables the capture of neuronal cells while maintaining their distinctive structures, such as long axons and dendrites. Many synaptic mRNAs are localized throughout the axonal and dendritic terminals, which are hundreds of micrometers distant from the neuronal cell body. For instance, representative postsynaptic mRNAs, such as *Psd95* and Homer1, are distributed widely from the neuronal cell body to the dendritic terminals (Cajigas et al., 2012). Additionally, presynaptic mRNAs, such as Synaptophysin and Synaptotagmin, are present exclusively in the developing growth cone, a specialized structure at the tip of the extending axon (Zivraj et al., 2010). Although the LMD method used in this study did not have sufficient precision in terms of the ability to dissect the axons and dendrites, we successfully identified the gene expression of these synaptic mRNAs in the engrafted NSPCs. More precise dissection with LMD must be developed for investigating distinct distribution of synaptic mRNAs in neuronal cells.

By performing selective molecular profiling with LMD, we were able to demonstrate that the expression of many pre- and postsynaptic molecules, including Bassoon, Piccolo, Synaptophysin, Synapsin, Synaptotagmin, *Vglut1*, *Vglut2*, *Vgat*, *Gad65*, *Gad67*, *Psd95*, Homer1, and Shank1, were observed in the engrafted NSPCs (Figures 4 and 5). In addition to the genes, a histological analysis confirmed that these synaptic molecules were observed in the neuronal endings of engrafted cells. Notably, the GFP-positive axons surrounded the host neurons and expressed presynaptic molecules, including BASSOON and VGLUT2 (Figure 4). Considering that these molecules are components of the presynaptic cytoskeletal matrix and are essential for neurotransmitter release at presynaptic terminals (Fenster et al., 2000; Südhof, 2013), these findings demonstrate that the engrafted NSPCs successfully communicated with the host neurons through synaptic organization. Moreover, postsynaptic molecules were identified at the dendrites of GFP-positive cells in the vicinity of the host neurons, suggesting that the engrafted NSPCs also received synaptic signals from the host neurons.

A recent report demonstrated that the selective depletion of synaptic vesicle-associated proteins within propriospinal circuits resulted in the impairment of upper limb motor performance (Kinoshita et al., 2012). They further showed that restoration of these synaptic proteins improved the deteriorated motor function, which suggests that the synaptic proteins play a pivotal role in the propriospinal system and motor function in the spinal cord. Similar to those findings, the reorganization of propriospinal circuits by synapse formation between the engrafted NSPCs and the host neurons improved the locomotor function after SCI in our study. Meanwhile, a significantly decreased number of synaptic boutons in the engrafted NSPCs, as well as less functional improvement, was observed in the setting of T9-neuronal ablation (Figures 2, 4, and 5). Although the correlation between the number of reorganized synaptic contacts and the extent of motor recovery after SCI remains unclear, synaptic facilitation could be one of the important determinants of the therapeutic efficacy of NSPC transplantation.

Several factors are considered to be required to promote synapse formation between engrafted NSPCs and host

neurons. First, the initial formation of each synapse depends on the physical contact between axons and dendrites (Cohen and Greenberg, 2008). Fares and colleagues reported that the optimal interneuronal distance for synapse formation is less than 50 μm (Fares and Stepanyants, 2009). Thus, the spatial proximity of neuronal cells is essential for synaptic integration. In fact, we could hardly observe the physical contact and synapse formation of the engrafted NSPCs between each other. Second, the secretion of guidance molecules, such as ephrin and neuroligin, was reported to accelerate the synaptic reorganization between neuronal cells (Bolsover et al., 2008). Notably, in the host neurons spared after SCI, upregulated expression of these molecules was observed (Jacobi et al., 2014). Selective host neuronal ablation abolished both the interneuronal spatial proximity and secretion of guidance molecules by host neurons, which may have decreased the synaptogenic potential and neuronal activity of the engrafted NSPCs in our study (Figures 3, 4, and 5).

Contrary to the findings in our experimental models, the toxin-receptor-mediated cell knockout (TRECK) method, in which most engrafted NSPCs are depleted, also abolished the functional improvement after NSPC transplantation (Abematsu et al., 2010; Cummings et al., 2005). These reports highlighted that the presence of engrafted NSPCs is critical to promote the functional recovery after SCI. On the other hand, our study indicated that the presence of spared host neurons affects the restorative potential of engrafted NSPCs, providing important insight for establishing therapeutic transplantation protocols for SCI. Considering our results and those of previous reports, a combination of neuroprotection by administrating neurohumoral factors and NSPC transplantation could, therefore, effectively promote functional recovery, even after severe SCI. Indeed, Lu and colleagues recently demonstrated that such combination therapy resulted in a significant improvement of functional recovery after SCI (Lu et al., 2012). They used neural stem cells with growth factor cocktails, including BDNF, NT3, PDGF, IGF, and HGF, which might have contributed to neuronal survival. Although transplanted NSPCs have been reported to secrete various neurohumoral factors (Kumamaru et al., 2012), our findings suggest that NSPC transplantation alone has limited efficacy for severe SCI.

In clinical studies, transplantation of neural stem cells has been applied for human cases of severe SCI; however, the therapeutic effects of NSPC transplantation are still controversial (Harrop et al., 2012). Seledtsova and colleagues transplanted human-derived NSPCs into the injured spinal cords of 43 patients, and nearly half of the patients (49%) showed some functional improvement after transplantation (Seledtsova et al., 2010). Although Dobkin and colleagues also transplanted human-derived NSPCs into the injured spinal cords of seven patients, none of these patients achieved a functional recovery after transplantation (Dobkin et al., 2006). These discrepancies regarding the efficacy of NSPC transplantation may be attributed to the differences in the severity of SCI in the study patients, because most of the SCI patients in Dobkin's study were classified into the American Spinal Injury Association (ASIA) Grade A (complete paralysis). In these patients, the paucity of remaining host neurons could underlie the inefficacy of NSPC transplantation for functional recovery. These findings caution against the use of injudicious transplantation protocols that do not adequately take into account the severity of the SCI.

In conclusion, we clarified the detailed synaptogenic profiles of engrafted NSPCs by LMD, and we determined the direct contributions of the host neurons and transplanted NSPCs to the reorganization of propriospinal circuits after NSPC transplantation. Our results clarified a mechanism underlying the functional recovery, which involves the reorganization of propriospinal circuits through synapse formation between engrafted NSPCs and host neurons after SCI. Protecting host neurons and facilitating the reorganization of propriospinal circuits are important strategies for improving the outcome following SCI, especially in cases with severe pathology. Analytical strategies using LMD will be useful in the field of stem cell biology, and our findings provide a better understanding of the therapeutic mechanism of stem cell transplantation in the injured CNS.

EXPERIMENTAL PROCEDURES

Animals

All animal studies were approved by the Committee of Ethics on Animal Experiment in Faculty of Medicine (A27-035-0), Kyushu University. Experiments were conducted in accordance with the institutional guidelines and regulations for animal experiments. The background strain of all mice (wild-type mice, CAG-EGFP transgenic mice, and ffLuc-cp156 mice) used in this study is C57BL/6, and the detailed information is described in the Supplemental Experimental Procedures.

NSPCs Primary Culture

Methods for the culture and expansion of NSPCs have been described previously (Okada et al., 2005), and the details are given in the Supplemental Experimental Procedures.

SCI and Cell Transplantation

Adult female C57BL/6 mice were anesthetized via an intraperitoneal injection of pentobarbital (75 mg/kg). SCI was induced at the ninth thoracic level using an Infinite Horizons impactor. After injury, 2 μl cell suspension (2.5×10^5 viable cells per microliter) was injected using a stereotaxic injector. The details are described in the Supplemental Experimental Procedures.

Behavioral Analysis

The motor functions were evaluated with the locomotor open-field rating scale on the BMS, the footprint analysis, and the grip walk test. The details are described in the Supplemental Experimental Procedures.

Histopathological Examination

After the mice were transcardially fixed with 4% paraformaldehyde, the spinal cord was removed, dehydrated, and embedded in OCT compound. The frozen tissues were cut in the sagittal or axial plane into 16-μm sections. The sections were subsequently stained with primary antibodies and then incubated with secondary antibodies or Hoechst. All antibodies used in this study are described in the Supplemental Experimental Procedures.

RT-PCR

RNA isolation and RT-PCR were performed as described previously (Kumamaru et al., 2012), and details are given in the Supplemental Experimental Procedures.

Image Acquisition and Quantitative Analysis

All images were obtained using an LSM510 laser-scanning microscope system (Zeiss) or a BZ-9000 digital microscope system (Keyence), and the details are described in the Supplemental Experimental Procedures.

SUPPLEMENTAL INFORMATION

Supplemental Information includes Supplemental Experimental Procedures, four figures, and one table and can be found with this article online at http://dx.doi.org/10.1016/j.stemcr.2015.06.004.

AUTHOR CONTRIBUTIONS

K.Y. designed and performed most of the experiments with technical help from K. Kobayakawa and K. Kubota. Y.O., H.O., A.M., and Y.I. provided experimental support and ideas for the project. S.O. designed the studies, supervised the overall project, and performed the final manuscript preparation.

ACKNOWLEDGMENTS

REFERENCES

Abematsu, M., Tsujimura, K., Yamano, M., Saito, M., Kohno, K., Kohyama, J., Namihira, M., Komiya, S., and Nakashima, K. (2010). Neurons derived from transplanted neural stem cells restore disrupted neuronal circuitry in a mouse model of spinal cord injury. J. Clin. Invest. *120*, 3255–3266.

Bareyre, F.M., Kerschensteiner, M., Raineteau, O., Mettenleiter, T.C., Weinmann, O., and Schwab, M.E. (2004). The injured spinal cord spontaneously forms a new intraspinal circuit in adult rats. Nat. Neurosci. *7*, 269–277.

Bolsover, S., Fabes, J., and Anderson, P.N. (2008). Axonal guidance molecules and the failure of axonal regeneration in the adult mammalian spinal cord. Restor. Neurol. Neurosci. *26*, 117–130.

Bradbury, E.J., and McMahon, S.B. (2006). Spinal cord repair strategies: why do they work? Nat. Rev. Neurosci. *7*, 644–653.

Cajigas, I.J., Tushev, G., Will, T.J., tom Dieck, S., Fuerst, N., and Schuman, E.M. (2012). The local transcriptome in the synaptic neuropil revealed by deep sequencing and high-resolution imaging. Neuron *74*, 453–466.

Cohen, S., and Greenberg, M.E. (2008). Communication between the synapse and the nucleus in neuronal development, plasticity, and disease. Annu. Rev. Cell Dev. Biol. *24*, 183–209.

Coleman, J.A., Harper, L.A., Perrin, P.B., Olivera, S.L., Perdomo, J.L., Arango, J.A., and Arango-Lasprilla, J.C. (2015). The relationship between physical and mental health variables in individuals with spinal cord injury from Latin America. PM R *7*, 9–16.

Conta, A.C., and Stelzner, D.J. (2004). Differential vulnerability of propriospinal tract neurons to spinal cord contusion injury. J. Comp. Neurol. *479*, 347–359.

Courtine, G., Song, B., Roy, R.R., Zhong, H., Herrmann, J.E., Ao, Y., Qi, J., Edgerton, V.R., and Sofroniew, M.V. (2008). Recovery of supraspinal control of stepping via indirect propriospinal relay connections after spinal cord injury. Nat. Med. *14*, 69–74.

Cummings, B.J., Uchida, N., Tamaki, S.J., Salazar, D.L., Hooshmand, M., Summers, R., Gage, F.H., and Anderson, A.J. (2005). Human neural stem cells differentiate and promote locomotor recovery in spinal cord-injured mice. Proc. Natl. Acad. Sci. USA *102*, 14069–14074.

Cusimano, M., Biziato, D., Brambilla, E., Donega, M., Alfaro-Cervello, C., Snider, S., Salani, G., Pucci, F., Comi, G., Garcia-Verdugo, J.M., et al. (2012). Transplanted neural stem/precursor cells instruct phagocytes and reduce secondary tissue damage in the injured spinal cord. Brain *135*, 447–460.

Dobkin, B.H., Curt, A., and Guest, J. (2006). Cellular transplants in China: observational study from the largest human experiment in chronic spinal cord injury. Neurorehabil. Neural Repair *20*, 5–13.

Doyle, J.P., Dougherty, J.D., Heiman, M., Schmidt, E.F., Stevens, T.R., Ma, G., Bupp, S., Shrestha, P., Shah, R.D., Doughty, M.L., et al. (2008). Application of a translational profiling approach for the comparative analysis of CNS cell types. Cell *135*, 749–762.

Fares, T., and Stepanyants, A. (2009). Cooperative synapse formation in the neocortex. Proc. Natl. Acad. Sci. USA *106*, 16463–16468.

Fenster, S.D., Chung, W.J., Zhai, R., Cases-Langhoff, C., Voss, B., Garner, A.M., Kaempf, U., Kindler, S., Gundelfinger, E.D., and Garner, C.C. (2000). Piccolo, a presynaptic zinc finger protein structurally related to bassoon. Neuron *25*, 203–214.

Flavell, S.W., and Greenberg, M.E. (2008). Signaling mechanisms linking neuronal activity to gene expression and plasticity of the nervous system. Annu. Rev. Neurosci. *31*, 563–590.

Flynn, J.R., Graham, B.A., Galea, M.P., and Callister, R.J. (2011). The role of propriospinal interneurons in recovery from spinal cord injury. Neuropharmacology *60*, 809–822.

Garg, A., Houlihan, D.D., Aldridge, V., Suresh, S., Li, K.K., King, A.L., Sutaria, R., Fear, J., Bhogal, R.H., Lalor, P.F., and Newsome, P.N. (2014). Non-enzymatic dissociation of human mesenchymal stromal cells improves chemokine-dependent migration and maintains immunosuppressive function. Cytotherapy *16*, 545–559.

Harrop, J.S., Hashimoto, R., Norvell, D., Raich, A., Aarabi, B., Grossman, R.G., Guest, J.D., Tator, C.H., Chapman, J., and Fehlings, M.G. (2012). Evaluation of clinical experience using cell-based therapies in patients with spinal cord injury: a systematic review. J. Neurosurg. Spine *17* (1, Suppl), 230–246.

Jacobi, A., Schmalz, A., and Bareyre, F.M. (2014). Abundant expression of guidance and synaptogenic molecules in the injured spinal cord. PLoS One *9*, e88449.

Kinoshita, M., Matsui, R., Kato, S., Hasegawa, T., Kasahara, H., Isa, K., Watakabe, A., Yamamori, T., Nishimura, Y., Alstermark, B., et al. (2012). Genetic dissection of the circuit for hand dexterity in primates. Nature *487*, 235–238.

Kobayakawa, K., Kumamaru, H., Saiwai, H., Kubota, K., Ohkawa, Y., Kishimoto, J., Yokota, K., Ideta, R., Shiba, K., Tozaki-Saitoh, H., et al. (2014). Acute hyperglycemia impairs functional improvement after spinal cord injury in mice and humans. Sci. Transl. Med. *6*, 256ra137.

Krueger, H., Noonan, V.K., Trenaman, L.M., Joshi, P., and Rivers, C.S. (2013). The economic burden of traumatic spinal cord injury in Canada. Chronic Dis. Inj. Can. *33*, 113–122.

Kumamaru, H., Ohkawa, Y., Saiwai, H., Yamada, H., Kubota, K., Kobayakawa, K., Akashi, K., Okano, H., Iwamoto, Y., and Okada, S. (2012). Direct isolation and RNA-seq reveal environment-dependent properties of engrafted neural stem/progenitor cells. Nat. Commun. *3*, 1140.

Lindvall, O., and Kokaia, Z. (2010). Stem cells in human neurodegenerative disorders—time for clinical translation? J. Clin. Invest. *120*, 29–40.

Lobo, M.K., Karsten, S.L., Gray, M., Geschwind, D.H., and Yang, X.W. (2006). FACS-array profiling of striatal projection neuron subtypes in juvenile and adult mouse brains. Nat. Neurosci. *9*, 443–452.

Lu, P., Wang, Y., Graham, L., McHale, K., Gao, M., Wu, D., Brock, J., Blesch, A., Rosenzweig, E.S., Havton, L.A., et al. (2012). Long-distance growth and connectivity of neural stem cells after severe spinal cord injury. Cell *150*, 1264–1273.

Mothe, A.J., and Tator, C.H. (2013). Review of transplantation of neural stem/progenitor cells for spinal cord injury. Int. J. Dev. Neurosci. *31*, 701–713.

Nishimura, S., Yasuda, A., Iwai, H., Takano, M., Kobayashi, Y., Nori, S., Tsuji, O., Fujiyoshi, K., Ebise, H., Toyama, Y., et al. (2013). Time-dependent changes in the microenvironment of injured spinal cord affects the therapeutic potential of neural stem cell transplantation for spinal cord injury. Mol. Brain *6*, 3.

Nori, S., Okada, Y., Yasuda, A., Tsuji, O., Takahashi, Y., Kobayashi, Y., Fujiyoshi, K., Koike, M., Uchiyama, Y., Ikeda, E., et al. (2011). Grafted human-induced pluripotent stem-cell-derived neurospheres promote motor functional recovery after spinal cord injury in mice. Proc. Natl. Acad. Sci. USA *108*, 16825–16830.

Okada, S., Ishii, K., Yamane, J., Iwanami, A., Ikegami, T., Katoh, H., Iwamoto, Y., Nakamura, M., Miyoshi, H., Okano, H.J., et al. (2005). In vivo imaging of engrafted neural stem cells: its application in evaluating the optimal timing of transplantation for spinal cord injury. FASEB J. *19*, 1839–1841.

Seledtsova, G.V., Rabinovich, S.S., Belogorodtsev, S.N., Parlyuk, O.V., Seledtsov, V.I., and Kozlov, V.A. (2010). Delayed results of transplantation of fetal neurogenic tissue in patients with consequences of spinal cord trauma. Bull. Exp. Biol. Med. *149*, 530–533.

Shah, P.K., Garcia-Alias, G., Choe, J., Gad, P., Gerasimenko, Y., Tillakaratne, N., Zhong, H., Roy, R.R., and Edgerton, V.R. (2013). Use of quadrupedal step training to re-engage spinal interneuronal networks and improve locomotor function after spinal cord injury. Brain *136*, 3362–3377.

Südhof, T.C. (2013). Neurotransmitter release: the last millisecond in the life of a synaptic vesicle. Neuron *80*, 675–690.

Tetzlaff, W., Okon, E.B., Karimi-Abdolrezaee, S., Hill, C.E., Sparling, J.S., Plemel, J.R., Plunet, W.T., Tsai, E.C., Baptiste, D., Smithson, L.J., et al. (2011). A systematic review of cellular transplantation therapies for spinal cord injury. J. Neurotrauma *28*, 1611–1682.

Volarevic, V., Erceg, S., Bhattacharya, S.S., Stojkovic, P., Horner, P., and Stojkovic, M. (2013). Stem cell-based therapy for spinal cord injury. Cell Transplant. *22*, 1309–1323.

Zivraj, K.H., Tung, Y.C., Piper, M., Gumy, L., Fawcett, J.W., Yeo, G.S., and Holt, C.E. (2010). Subcellular profiling reveals distinct and developmentally regulated repertoire of growth cone mRNAs. J. Neurosci. *30*, 15464–15478.